

SAND97-1466C

CONF-970805--3

**CHEMICAL CLASS SPECIFICITY USING SELF-ASSEMBLED  
MONOLAYERS ON SAW DEVICES:  
EFFECTS OF ADSORPTION TIME AND SUBSTRATE GRAIN SIZE**

**R. C. Thomas, A. J. Ricco,<sup>\*,†</sup> and C. R. DiRubio**

*Microsensor R&D Department  
Sandia National Laboratories  
Albuquerque, NM 87185-1425*

**H. C. Yang and R. M. Crooks\***

*Department of Chemistry  
Texas A&M University  
College Station, TX 77843-3255*

\*Authors to whom correspondence should be addressed

<sup>†</sup>ajricco@sandia.gov

**ABSTRACT**

We report selectivity and sensitivity for 97-MHz SAW (surface acoustic wave) sensors functionalized with  $(\text{COO}^-)_2/\text{Cu}^{2+}$ -terminated, organomer-captan-based, self-assembled monolayers (SAMs). Responses were obtained as a function of SAM formation time on thin Au films of controlled grain size. We find that the SAM films (1) preferentially adsorb classes of organic analytes according to simple chemical interaction concepts, (2) reversibly adsorb multilayers of some analytes well below their saturation vapor pressure, (3) adsorb more diisopropylmethylphosphonate (DIMP) at a given partial pressure as SAM solution-phase adsorption time increases, and (4) adsorb more DIMP at a given partial pressure as the grain size of the supporting Au film decreases.

**INTRODUCTION**

Chemically sensitive SAW devices provide a basis to design sensors for specific analytes. Custom-synthesized molecular recognition sites offer one solution, but this approach is time-intensive and hampered by the large number of molecules for which chemical sensors are sought. In addition, nonspecific physical adsorption may thwart the selectivity of the most elegantly conceived guest-host complexes. Our approach is to relax selectivity requirements significantly, using arrays of multiple sensors with partial

DISTRIBUTION OF THIS DOCUMENT IS UNLIMITED.

ng  
**MASTER**

selectivity and relying on the analyte-dependent "fingerprint" provided by the response pattern for molecular or class identification.

We base our design of moderately selective interfaces upon known, reversible, bulk-phase interactions between analytes and functional groups that can be incorporated into a thin film (1-3). Composite SAM films based on organomercaptans provide a simple methodology for fabricating a range of such vapor/solid interfaces differing in terminal functionalities but related by similar surface coverage, structure, and orientation (4). Even with different substrate materials, grain sizes, and surface roughness, the ordering of the S head group onto the predominant (111) Au crystallite orientation, along with the close-packed self assembly of the alkane tails, yields relatively consistent characteristics.

Nevertheless, subtle effects, such as the number of defects in a SAM film, may result from differences in the Au film's underlying microstructure, presumably associated with grain boundaries (5,6). The role of SAM adsorption time is also an issue: a specific defect structure reportedly forms for SAM films prepared using solution-phase adsorption times of 24 to 48 h (7,8). Moreover, a recent STM study shows that Au surfaces reorganize over several days in the presence of thiols; many days are required to complete the self-assembly process under some conditions (9).

SAW devices are exceptionally sensitive to surface adsorbates (10): our minimum-detectable mass change is 100 pg/cm<sup>2</sup>. Often, SAW velocity is perturbed in proportion to surface mass loading, in which case measured frequency shift is directly proportional to changes in mass/area (10). When they occur, changes in the mechanical properties of a thin-film coating often result in both attenuation of the acoustic wave and a change in SAW velocity (10-12).

A SAW sensor functionalized with an organomercaptan SAM having a carboxylate-coordinated Cu<sup>2+</sup> endgroup (hereafter, "Cu<sup>2+</sup>-SAM") reversibly responds to organophosphonates (1,2). In this paper, we compare the SAW response from a Cu<sup>2+</sup>-SAM and a methyl-terminated SAM to a vapor-phase organophosphonate and several volatile organic compounds (VOCs). We explore in detail the dependence of the extent of adsorption upon variations in solution-phase SAM adsorption time and the grain size of the supporting Au surface.

## RESULTS AND DISCUSSION

### Chemical Specificity

Experimental details and additional results can be found in the literature (1). Figure 1 shows SAW response vs. vapor-phase concentration for six different VOCs and water interacting with a  $\text{Cu}^{2+}$ -SAM-covered device; the data have been converted from frequency shift to adsorbate molecules/area. The data indicate preferential adsorption of DIMP and acetone, followed by water, *n*-propanol, trichloroethylene (TCE), and toluene; *i*-octane scarcely adsorbs. The first four of these molecules are Lewis bases, with oxygen lone pairs likely to interact with the Lewis acid  $\text{Cu}^{2+}$  that terminates the  $\text{Cu}^{2+}$ -SAM. Weaker interactions might be expected between  $\text{Cu}^{2+}$  and the chlorine atoms of TCE, as well as the  $\pi$  electron cloud of toluene. Only van der Waals interactions are possible between *i*-octane and this SAM.

In contrast to the  $\text{Cu}^{2+}$ -SAM results, Figure 2 shows SAW adsorption isotherms for the same set of VOCs interacting with a SAM formed from  $\text{CH}_3(\text{CH}_2)_{15}\text{SH}$  (" $\text{CH}_3$ -SAM") SAM. Surprisingly, the preference of this film, particularly at high analyte concentrations, is for the adsorption of acetone and water. With no particular interaction expected between the  $\text{CH}_3$ -SAM and polar species, we believe the tendency of  $\text{H}_2\text{O}$  to form H-bonded networks with itself to be the most likely explanation for its relatively large response. *A priori*, a similar effect is not expected for acetone, which has no H-bonding protons. However, the acetone was not dried, so the entrained vapor undoubtedly contains some amount of water vapor, which could participate in the formation of a H-bonded network, promoting multilayer adsorption. A second possibility involves grain-boundary adsorption: defects in the SAM necessarily occur at Au grain boundaries, perhaps exposing sulfur head groups and/or forming "cracks" that are attractive to molecules with the appropriate size, shape, and chemical properties. In either case, we believe that the extensive adsorption is not chemically specific to this particular SAM.

We examine the degree to which surface/adsorbate interactions are specific to a particular SAM tail group by examining the difference between the responses of the  $\text{Cu}^{2+}$ -SAM and  $\text{CH}_3$ -SAM. The differences between the isotherms of Figures 1 and 2 are plotted in Figure 3. These data show a marked preference for the adsorption of DIMP relative to the other compounds, indicative of specific interactions between DIMP and the  $\text{Cu}^{2+}$ -SAM. In marked contrast, the rather large responses to acetone and water displayed by the individual SAMs (Figs. 1 and 2) are not specific: they largely cancel in the difference plot of Figure 3. In addition, the  $\text{Cu}^{2+}$ -SAM shows about three times the response for propanol, due to interaction between the alcohol  $-\text{OH}$  and the  $\text{Cu}^{2+}$ , compared to the  $\text{CH}_3$ -SAM. In the case of *i*-octane, the difference is negative, consistent the more favorable interaction being between this molecule and the similarly nonpolar  $\text{CH}_3$ -SAM.

## Multilayer Adsorption

The data in Figure 1 indicate that multilayers form (based on molar volumes from the bulk liquids) at  $p/p_{\text{sat}} = 0.5$  for all the analytes but *i*-octane. The number of multilayers indicates qualitatively the "range" of SAM/analyte interactions. The fact that ca. 17 layers of DIMP adsorb at  $p/p_{\text{sat}} = 0.5$  is consistent with our conclusion from Figure 3 that this analyte interacts most strongly and specifically with the  $\text{Cu}^{2+}$ -SAM. The next-highest equivalent mass coverage for an analyte at  $p/p_{\text{sat}} = 0.5$  is about 9 layers for acetone, which the results in Figure 3 suggest is a nonspecific sorption process. The coverage of water is about 3 layers at this  $p/p_{\text{sat}}$  (also relatively nonspecific). We conclude that DIMP is by far the most amenable species to ordering-induced multilayer formation. Importantly, the multilayer formation (for all analytes examined) is fully reversible: purging with pure  $\text{N}_2$  returns the SAW frequency shift to zero.

The results presented in the next two sections are consistent with the notion that analyte multilayer formation results from molecular ordering induced by the SAM: the solution-phase formation time of the SAM, as well as the grain size of the supporting Au surface, are shown to influence dramatically the extent of multilayer formation.

## Dependence on SAM Formation Time

Figure 4 presents a series of DIMP adsorption isotherms obtained from SAW devices functionalized with  $\text{Cu}^{2+}$ -SAMs adsorbed from ethanolic solutions of 0.5 mM mercaptoundecanoic acid (MUA) for times of 36, 84, or 180 h; the  $\text{Cu}^{2+}$  is coordinated after MUA adsorption by a 10-min immersion in 2 mM  $\text{Cu}(\text{ClO}_4)_2 \cdot 6\text{H}_2\text{O}$  in ethanol. The polycrystalline Au films upon which the SAMs were formed have an average Au grain size of 50 nm (1). The binding affinity of the  $\text{Cu}^{2+}$ -SAM for DIMP increases dramatically with MUA monolayer formation time.

Extended adsorption times probably affect the alkane portion of the MUA SAM, which in turn influences the orientation of the carboxylate end groups and the coordinated  $\text{Cu}^{2+}$ . Previous reports show that the alkane portion of MUA monolayers are "liquid-like" after adsorbing for 10 – 36 h (13,14); the hydrocarbon chain may become more "crystalline" with increasing adsorption time (9). In addition to orientation effects, carboxylic acid-terminated SAMs can exhibit extensive intramonolayer hydrogen bonding (15,16); an extensive H-bonding structure formed over long adsorption times might lead to a  $(\text{COO}^-)_2/\text{Cu}^{2+}$  interface more favorable to ordering of adsorbed DIMP. The long adsorption times we use can be likened to a long-duration, low-temperature anneal, avoiding the difficulty of increasing porosity that is associated with post-SAM-formation thermal annealing (1,7,8,17).

SAW attenuation data (not shown) obtained during the three DIMP adsorption isotherms of Figure 4 reveal appreciable attenuation only for the SAM prepared for 180

h (1), a definite indication that this film differs in its structural/mechanical properties from the others. Supporting ellipsometric measurements indicate that the thickness of all three composite SAMs represented in Figure 4 is  $1.9 \pm 0.5$  nm (1): the Cu-SAM is only a single monolayer thick, regardless of adsorption time.

### Gold Grain-Size Effects

The thin Au films that support the  $\text{Cu}^{2+}$ -SAMs were produced with a range of grain sizes, characterized by constant-repulsive-force atomic force microscopy (1). The 100 nm-thick Au films were electron-beam evaporated, without an adhesion layer, onto SAW quartz substrates maintained at: room-temperature; 100 °C followed by a 2-h anneal at 150 °C; and 100 °C followed by a 2-h anneal at 250 °C. The average grain sizes produced by the respective deposition/anneal conditions were 50, 80, and 240 nm. Surface roughness was  $1.1 \pm 0.1$  nm for the three different films.

Figure 5 shows DIMP adsorption isotherms for  $\text{Cu}^{2+}$ -SAMs prepared using 180-h MUA adsorption times on the variable-grain-size Au surfaces. As the grain size of the Au film *decreases*, there is a significant *increase* in the extent of adsorption of DIMP at a given  $p/p_{\text{sat}}$ . Neither surface roughness nor surface coverage by the SAMs varies sufficiently to explain the factor-of-2.5 variation in DIMP adsorption measured  $p/p_{\text{sat}} = 0.5$  (1, 18). Rather, we believe grain size affects the nature and extent of ordering of the  $\text{Cu}^{2+}$ -SAMs.

We have observed similar grain-size effects for MUA film-formation times of 36 or 84 h, but the effect is most pronounced for the 180-h formation time. Furthermore, our results show the least sample-to-sample variation for the smallest grains.

## CONCLUSIONS

Our results show that a pair of SAM-functionalized SAW sensors, one bearing a methyl- and the other a  $(\text{COO}^-)_2/\text{Cu}^{2+}$ -terminated monolayer, differentiate between chemically specific and nonspecific adsorption. The results further show that the  $\text{Cu}^{2+}$ -SAM films (1) preferentially adsorb particular classes of organic analytes in a manner that follows from simple concepts such as Lewis acid/base, H-bonding, and polar vs. nonpolar interactions, (2) readily and reversibly adsorb the equivalent of 10 - 20 layers of some analytes at  $p/p_{\text{sat}} = 0.5$ , (3) adsorb a greater quantity of DIMP at a given partial pressure for longer solution-phase formation times of the organomercaptan monolayer, and (4) adsorb a greater quantity of DIMP at a given partial pressure as the grain size of the supporting Au film decreases. Result (1) is straightforward and to be expected, but we believe results (2) - (4) are consequences of the extent and nature of the ordering of the SAM and its outer surface: the ordering affects the thermodynamics of adsorption of multilayers of analyte.

## ACKNOWLEDGMENTS

R. C. T. and A. J. R. acknowledge the excellent technical assistance of Al Staton and Mary-Anne Mitchell. R. M. C. and H. Y. gratefully acknowledge the National Science Foundation (CHE-9313441) and the United States Dept. of Energy under a contract from Sandia National Laboratories for support. Sandia National Laboratories is supported by the United States Department of Energy under Contract DE-AC04-94AL85000. Sandia is a multiprogram laboratory operated by Sandia Corporation, a Lockheed-Martin Company, for the United States Department of Energy.

## REFERENCES

1. R. C. Thomas, H. C. Yang, C. R. DiRubio, A. J. Ricco, and R. M. Crooks, *Langmuir*, **12**, 2239 (1996).
2. L. J. Kepley, R. M. Crooks, and A. J. Ricco, *Anal. Chem.*, **64**, 3191 (1992).
3. R. C. Ebersole, J. A. Miller, J. R. Moran, and M. D. Ward, *J. Am. Chem. Soc.*, **112**, 3239 (1990); C. A. Mirken and M. S. Wrighton, *J. Am. Chem. Soc.*, **112**, 8596 (1990); S. Steinberg and I. Rubinstein, *Langmuir*, **8**, 1183 (1992).
4. R. G. Nuzzo and D. L. Allara, *J. Am. Chem. Soc.*, **105**, 4481 (1983); C. D. Bain, E. B. Troughton, Y.-T. Tao, J. Evall, G. M. Whitesides, and R. G. Nuzzo, *J. Am. Chem. Soc.*, **111**, 321 (1989) and references therein; L. H. Dubois and R. G. Nuzzo, *Annu. Rev. Phys. Chem.*, **43**, 437 (1992) and references therein.
5. L.-H. Guo, J. S. Facci, G. McLendon, and R. Mosher, *Langmuir*, **10**, 4588 (1994).
6. S. E. Creager, L. A. Hockett, and G. K. Rowe, *Langmuir*, **8**, 854 (1992).
7. P. Fenter, P. Eisenberger, and K. S. Liang, *Phys. Rev. Lett.*, **70**, 2447 (1993).
8. N. Camillone III, C. E. D. Chidsey, P. Eisenberger, P. Fenter, J. Li, K. S. Liang, G.-Y. Liu, and G. Scoles, *J. Phys. Chem.*, **99**, 744 (1993).
9. G. E. Poirier and M. J. Tarlov, *J. Phys. Chem.*, **99**, 10960; 10966 (1995).
10. D. S. Ballantine, R. M. White, S. J. Martin, A. J. Ricco, G. C. Frye, E. T. Zellers, and H. Wohltjen, *Acoustic Wave Sensors: Theory, Design, and Physico-Chemical Applications*, Academic Press, San Diego (1997).
11. S. J. Martin, G. C. Frye, and S. D. Senturia, *Anal. Chem.*, **66**, 2201 (1994).
12. S. J. Martin and A. J. Ricco, *Sens. Actuators*, **A22**, 712 (1990).
13. L. Sun, L. J. Kepley, and R. M. Crooks, *Langmuir*, **8**, 2101 (1992).
14. E. L. Smith, C. A. Alves, J. W. Anderegg, and M. D. Porter, *Langmuir*, **8**, 2707 (1992).
15. L. Sun, R. M. Crooks, and A. J. Ricco, *Langmuir*, **9**, 1775 (1993).
16. R. G. Nuzzo, L. H. Dubois, and D. L. Allara, *J. Am. Chem. Soc.*, **112**, 558 (1990).
17. N. Camillone III, P. Eisenberger, T. Y. B. Leung, P. Schwartz, G. Scoles, G. E. Poirier, and M. J. Tarlov, *J. Phys. Chem.*, **101**, 11031 (1994).
18. Y. Golan, L. Margulis, and I. Rubinstein, *Surf. Sci.*, **264**, 312 (1992).

## DISCLAIMER

This report was prepared as an account of work sponsored by an agency of the United States Government. Neither the United States Government nor any agency thereof, nor any of their employees, makes any warranty, express or implied, or assumes any legal liability or responsibility for the accuracy, completeness, or usefulness of any information, apparatus, product, or process disclosed, or represents that its use would not infringe privately owned rights. Reference herein to any specific commercial product, process, or service by trade name, trademark, manufacturer, or otherwise does not necessarily constitute or imply its endorsement, recommendation, or favoring by the United States Government or any agency thereof. The views and opinions of authors expressed herein do not necessarily state or reflect those of the United States Government or any agency thereof.

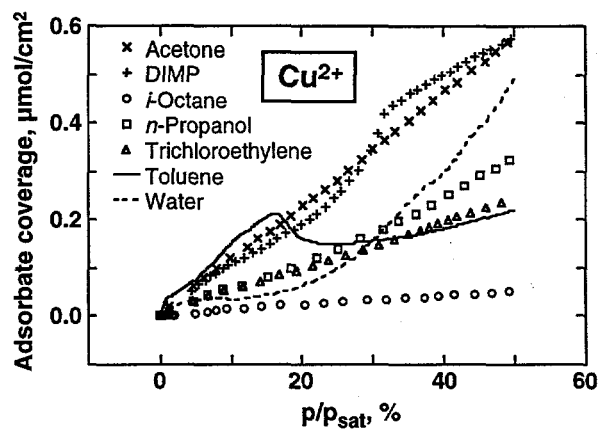


Figure 1. SAW-measured adsorption isotherms for several organic vapors on a  $(\text{COO}^-)_2/\text{Cu}^{2+}$ -terminated SAM.

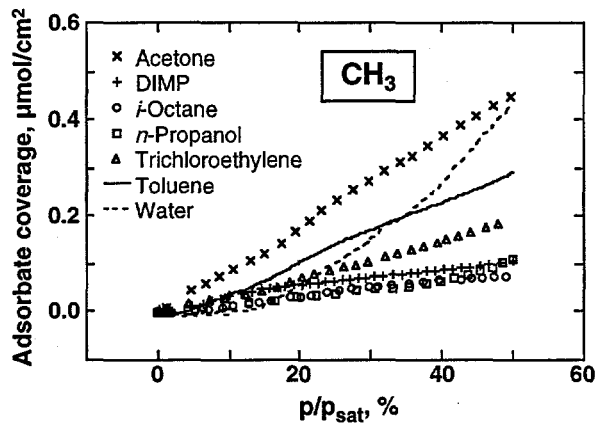


Figure 2. SAW-measured adsorption isotherms for several organic vapors on a  $\text{CH}_3$ -terminated SAM.

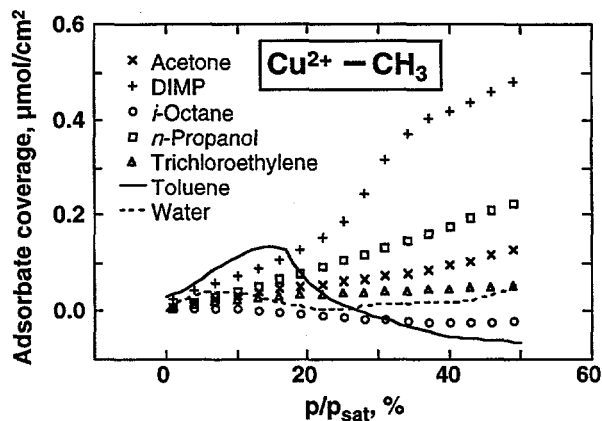
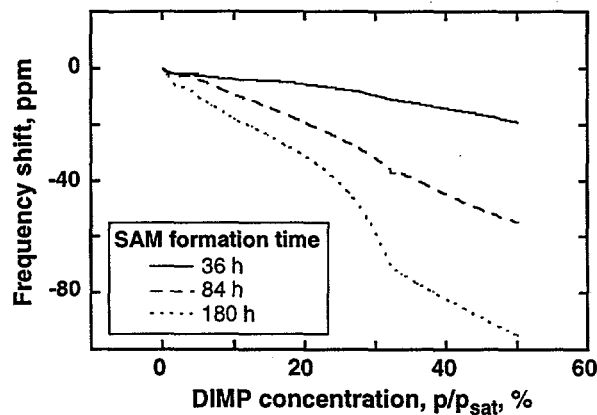
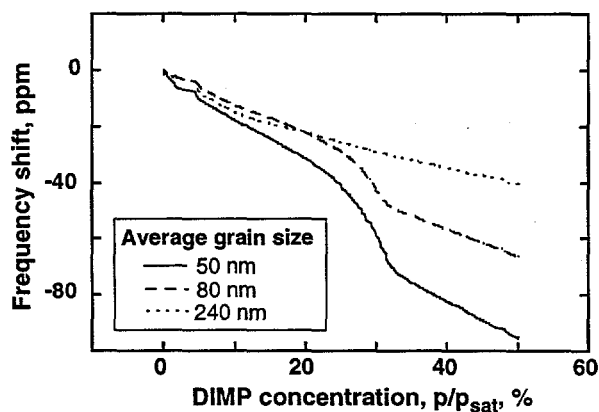


Figure 3. Difference between the isotherms of Figures 1 and 2 as a function of adsorbate partial pressure.



*Figure 4. DIMP adsorption isotherms for  $\text{Cu}^{2+}$ -SAM-functionalized SAW devices. The SAMs were formed using variable solution-phase adsorption times as indicated. Increased adsorption results from enhanced ordering at the vapor/solid interface.*



*Figure 5. DIMP adsorption isotherms for  $\text{Cu}^{2+}$ -SAMs prepared on Au surfaces with variable grain size; the extent of adsorption increases as grain size decreases. The differences are NOT attributable to surface roughness.*

**DISCLAIMER**

**Portions of this document may be illegible  
in electronic image products. Images are  
produced from the best available original  
document.**